Chapter 7 Cosmology with the cosmic microwave background

Chapter 1 introduced you to the basic properties of CMB radiation and its importance as a tool for understanding the Universe, and in Chapter 6 you learned more about the observational properties of the CMB and the mathematical methods used to describe and model it. This chapter will focus on the physical processes that produce the observed anisotropies in the CMB and how cosmologists use CMB observations – and measurements of the angular power spectrum in particular – to measure cosmological density parameters such as Ω_{m} and Ω_{b}.

Objectives

Working through this chapter will enable you to:

- explain how physical processes operating before the epoch of last scattering produced the different features we observe in the CMB angular power spectrum
- explain how perturbations in the distributions of matter and radiation in the early Universe imprinted small fluctuations in the temperature of the CMB that we can still observe today
- understand how the values of the cosmological parameters impact the observable properties of the CMB
- explain how various CMB properties would change if the cosmological parameters had different values from those we actually measure for the real Universe
- understand the ways in which cosmologists derive cosmological parameter constraints from very precise observations of the CMB
- understand that CMB observations have some limitations as probes to measure the cosmological parameters but these can often be overcome by simultaneously considering observations of other astrophysical phenomena, such as Type Ia supernovae.

7.1 Explaining the CMB angular power spectrum

The CMB power spectrum shown in Figure 7.1 is exactly the same as the one you saw in Figure 6.13. As in the previous instance, the black points show the measurements and their associated errors. Note the effect of cosmic variance in the increased scatter at larger angular scales. As before, the blue line shows the theoretical model that best fits the observed data.

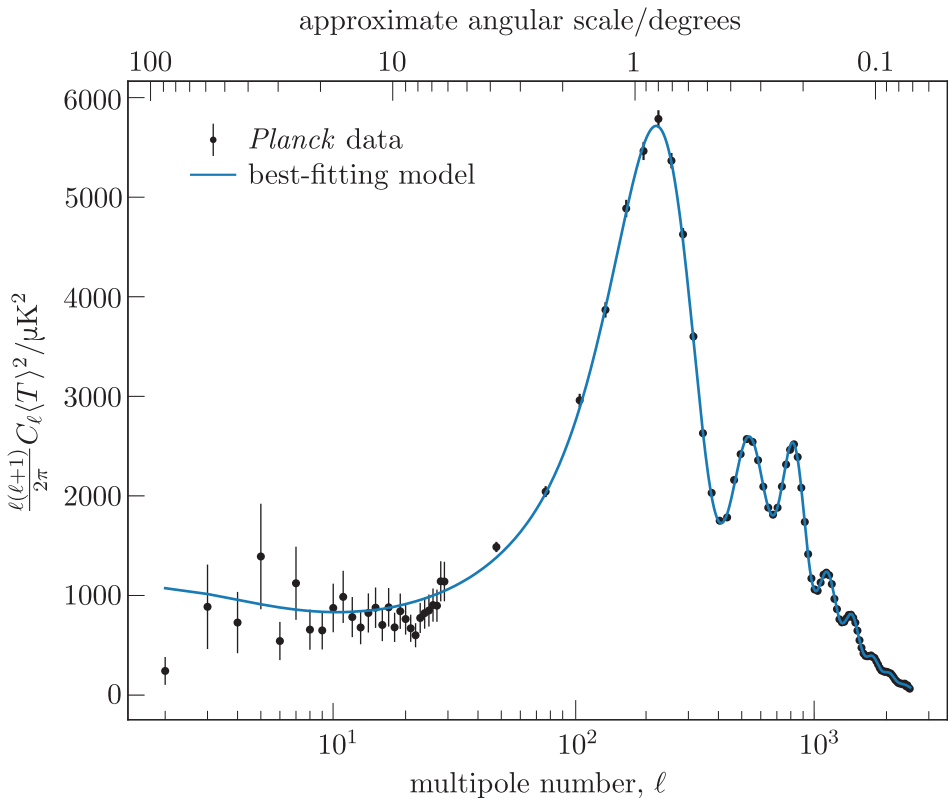

Figure 7.1 The CMB angular power spectrum measured by the *Planck* satellite.

In this section we will examine the structure of the CMB angular power spectrum in much more detail. The different features we investigate will help us to understand the physical processes that were operating before the epoch of last scattering and provide constraints on the values of several cosmological parameters.

To understand why the CMB angular power spectrum exhibits the features that it does, it is important to remember that the *temperature* fluctuations that we observe in the CMB reflect fluctuations in the *density* of the Universe at the epoch of last scattering.

7.1.1 Before the epoch of last scattering

Many cosmological theories predict *primordial* perturbations in the densities of matter and radiation and, further, that these perturbations have equal variance on all physical scales. If this primordial distribution of density perturbations persisted until the epoch of last scattering, then we would expect the values of Δ_T^2 observed in the power spectrum to be equal and independent of the multipole number, ℓ. However, this expectation is not consistent with the complex pattern of peaks in Figure 7.1. Instead, we can see that by the epoch of last scattering, the variance of the density fluctuations had become much larger on some physical size scales while the amplitudes of fluctuations on other scales were correspondingly reduced.

To help us understand how the primordial pattern of density perturbations evolved to produce the CMB angular power spectrum that we *do* observe, we will construct a simplified model for the contents of the early Universe. At the epoch of last scattering, the density parameter for the cosmological constant (Ω_Λ) was almost 10 orders of magnitude smaller than those of either matter (Ω_m) or radiation (Ω_r), so we can neglect its influence in our simple model. The early Universe also contained neutrinos, but their energy density was approximately half that of the photons and they interact so weakly with other components that their influence can also be ignored. We are left with components of radiation and matter, and we will subdivide the latter into baryonic matter and dark matter.

As soon as the primordial density fluctuations appeared, the contents of the Universe began to move under the influence of gravity. The amplitudes of the density perturbations began to increase as dark matter, photons and baryons fell into gravitational potential wells associated with denser-than-average regions of the Universe (often referred to as 'overdensities'), leaving behind other regions that became correspondingly less dense.

The gravitational influences of matter and radiation do not propagate instantaneously. In fact, the general theory of relativity predicts that information about the distribution of energy density in the universe is transmitted by gravitational waves that propagate at the speed of light. This means that by the epoch of last scattering, the largest structures that would have had time to respond gravitationally to the primordial density fluctuations would have had sizes comparable to the horizon distance at that time:

The existence of gravitational waves has now been observationally verified by observatories such as Advanced LIGO and Virgo.

$$d_\mathrm{hor}(t_\mathrm{ls}) = a(t_\mathrm{ls})c\int_0^{t_\mathrm{ls}} \frac{\mathrm{d}t}{a(t)} \tag{7.1}$$

Any primordial density perturbations with physical sizes larger than $d_\mathrm{hor}(t_\mathrm{ls})$ at the epoch of last scattering would not have had time to evolve in this way and should therefore have *retained* their primordial spatial power spectrum.

To calculate a value for the horizon distance in our simplified model Universe by hand, we would need an expression for the scale factor $a(t)$. However, the resulting expression is very complicated and obtaining it

analytically is not straightforward. Instead, try the following Python example, which will take you through the steps needed to compute $d_{\rm hor}(t_{\rm ls})$ *numerically*.

Example 7.1

Using the techniques you learned during the first week-long Python practical activity, write a short program to numerically integrate the Friedmann equation and show that the horizon distance at the epoch of last scattering $d_{\rm hor}(t_{\rm ls}) = 0.29\,{\rm Mpc}$.

Solution

Please refer to the Example 7.1 Jupyter Notebook in the online module resources to see the solution to this example.

In Example 6.2 you saw that we can use the angular diameter distance $d_{\rm A}(z_{\rm ls})$ to relate the size of structures on the surface of last scattering to their apparent angular size when observed from Earth. For structures with a physical size equal to the horizon distance at that time, $d_{\rm hor}(t_{\rm ls})$, the corresponding angular size will be

$$\theta_{\rm hor}(z_{\rm ls}) = \frac{d_{\rm hor}(t_{\rm ls})}{d_{\rm A}(z_{\rm ls})} = \frac{0.29\,{\rm Mpc}}{12.73\,{\rm Mpc}} = 0.023\,{\rm rad} \approx 1.3^\circ$$

- To what value of ℓ does an angular size of 1.3° approximately correspond?

- An angular size of 1.3° corresponds to $\ell \approx 180^\circ/1.3^\circ \approx 140$.

Recall that the normalisation factor of $\ell(\ell+1)$ in Equation 6.10 is engineered to ensure that primordial density perturbations with a scale-free spatial power spectrum produce a CMB angular power spectrum with an approximately constant value for Δ_T for all values of ℓ. Therefore we would expect the graph in Figure 7.1 to approximate a horizontal line for temperature fluctuations that reflect density perturbations larger than the horizon distance (sometimes referred to as 'super-horizon' perturbations), and which correspond to values of ℓ less than $\sim$140.

In reality, the graph does not completely flatten out until $\ell \lesssim 40$, which reflects the fact that $d_{\rm hor}(t_{\rm ls})$ is not a hard cut-off and density perturbations larger than the horizon distance would still have evolved slightly prior to the epoch of last scattering. The flat region of the CMB power spectrum below $\ell \approx 40$ is called the **Sachs–Wolfe plateau** in honour of the two scientists, Rainer K. Sachs and Arthur M. Wolfe, whose theoretical predictions helped to explain its existence.

7.1.2 Acoustic oscillations

Primordial perturbations that were smaller than $d_{\rm hor}(t_{\rm ls})$ at the epoch of last scattering underwent a very different evolutionary history from those on super-horizon scales. Bear in mind that the horizon distance grows larger as the Universe expands, so density perturbations that were smaller than $d_{\rm hor}(t_{\rm ls})$ at the epoch of last scattering may, at earlier times, have been larger than the horizon distance. Smaller perturbations would have been encompassed earlier by the expanding particle horizon and, therefore, would have been evolving for longer at the epoch of last scattering. In fact, the details of a particular perturbation's evolution depend on whether the energy density of the Universe was dominated by matter or radiation when the particle horizon expanded to encompass it.

Exercise 7.1

Consider a universe that contains only matter and radiation. Such a universe is a good model for the real Universe early in its history, when Ω_Λ was negligible. The age $t(a)$ of this universe corresponding to some arbitrarily chosen scale factor, a, can be expressed in terms of the scale factor $a_{\rm mr}$ at the particular instant when the density parameters of matter and radiation were equal:

$$t(a) = \frac{4}{3}\frac{a_{\rm mr}^2}{H_0\sqrt{\Omega_{\rm r,0}}}\left[1-\left(1-\frac{a}{2a_{\rm mr}}\right)\left(1+\frac{a}{a_{\rm mr}}\right)^{1/2}\right] \tag{7.2}$$

Using this expression and assuming that the epoch of matter–radiation equality occurred at redshift $z_{\rm mr} \approx 5730$, show that by the epoch of last scattering at $z_{\rm ls} \approx 1090$ the energy density of this universe had been dark-matter-dominated for just over 94% of its history.

In Chapter 6 you read that before the epoch of last scattering, the opacity of the Universe was very high. This resulted in continuous Thomson scattering between high-energy photons and free electrons, which produced a coupling between the radiation and baryonic matter components that was so strong that they effectively behaved like a single fluid. This medium is sometimes referred to as the **photon–baryon fluid**

In Exercise 7.1 you showed that at the epoch of last scattering, the energy density of the Universe would have been dominated by dark matter for ∼90% of its history. The photon–baryon fluid within any density perturbations enveloped by the particle horizon during this time can therefore be considered to have been evolving in a gravitational potential well that was dominated by the influence of dark matter.

Figure 7.2 illustrates how the dark matter drew the photons and baryons with it into the primordial overdensities as they grew. As photons and baryons became concentrated in the evolving overdensities, their temperatures and Thomson scattering rates increased, resulting in

increased internal pressure. Eventually the pressure in the photon–baryon fluid became large enough to counteract the gravitational influence of the dark matter and the fluid began to expand out of the overdense regions at the speed of sound.

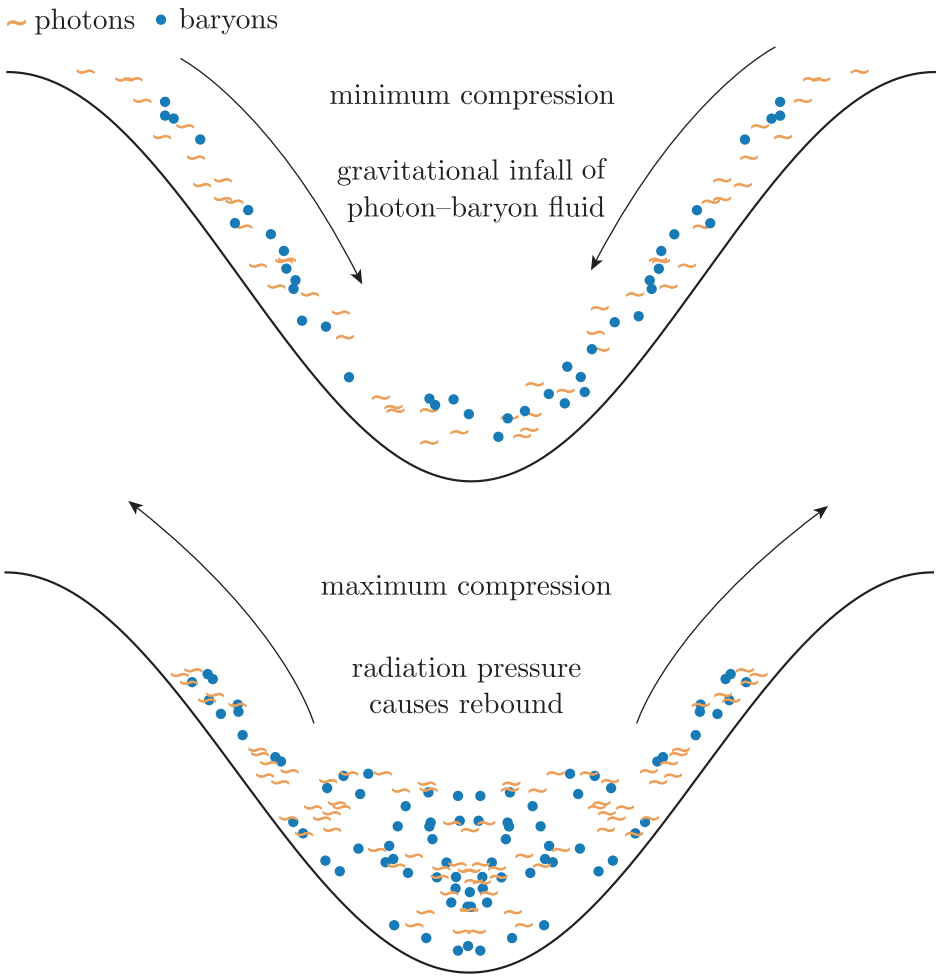

Figure 7.2 Diagram showing how photons and baryons move in the region around a dark-matter overdensity. In the upper panel, a low-pressure photon–baryon fluid begins falling into the gravitational potential well created by the dark matter. As it does so, the internal pressure in the photon–baryon fluid starts to increase. In the lower panel, the radiation pressure has increased so much that it can resist the gravitational influence of the dark matter and the photon–baryon fluid rebounds and expands out of the overdensity at the speed of sound.

- How do you think the expansion of the photon–baryon fluid affected the overall growth of a density perturbation like the one sketched in Figure 7.2 during the matter-dominated era of the Universe's history?
- The growth of such density perturbations was strongly dominated by the gravitational influence of the dark matter they contained, so the motion of the photons and baryons had almost no influence at all.

As the photon–baryon fluid expanded, its temperature decreased and its internal pressure dropped until it could no longer resist the gravitational influence of the dark matter and the fluid began to fall inward again. This process led to repeated cycles of expansion and collapse that continued until the photons and baryons decoupled, around the epoch of last scattering.

These cycling density and pressure perturbations are the acoustic oscillations that were first introduced in the previous chapter. They are responsible for the peaks that we observe in Figure 7.1. For this reason, the peaks in the CMB power spectrum are often called **acoustic peaks**. You may also see them referred to as *Doppler peaks* but, as we will notice later in the chapter, this is something of a misnomer.

Numerical labels for the acoustic peaks

The acoustic peaks are conventionally labelled using cardinal numbers in order of increasing ℓ. For example, the peak at $\ell \approx 200$ is called the *first* peak, the peak at $\ell \approx 500$ is called the *second* peak, and so on. Later in this chapter we will reference these numerical labels when we discuss the sets of odd- and even-numbered peaks.

In general, the odd-numbered peaks represent oscillations at maximum compression, and the even-numbered peaks correspond to oscillations that are at maximum expansion. By measuring the heights and positions of the different peaks in the CMB power spectrum, cosmologists can derive strong constraints for several cosmological parameters.

A landscape of wells and hills

So far in this section our discussion has focused primarily on regions of the Universe that are denser than average. These overdensities produce gravitational potential wells throughout the Universe. However, when thinking about acoustic oscillations you should keep in mind that for every overdense potential *well* there is a neighbouring potential *hill*, corresponding to a region of the Universe that is less dense than average.

As photons, baryons and dark matter fall into potential wells and increase their density, they are falling from the surrounding potential hills, thereby reducing the density of the latter even further. If we focus on acoustic oscillations with a particular physical scale, the pattern they make throughout the Universe is somewhat like a landscape filled with adjacent *three-dimensional* potential wells and hills, with the photon–baryon fluid sloshing between them.

Figure 7.3 (overleaf) shows a simple representation of this concept in one dimension.

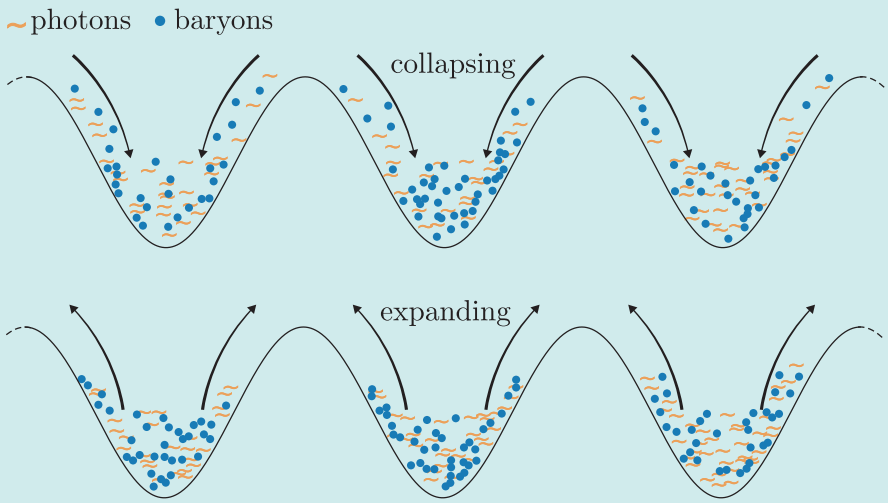

Figure 7.3 Simple one-dimensional illustration showing the landscape of potential wells and hills with the photon–baryon fluid moving within it. In the upper panel the photons and baryons fall from the hills into the wells, and in the lower panel the compressed photon–baryon fluid expands out of the wells and up onto the hills.

However, it is important to remember that this analogy is not perfect. Acoustic oscillations were happening throughout the Universe on *all* physical scales, with smaller oscillations evolving within larger ones. The complex pattern that we observe in the CMB results from the superposition of all these overlapping oscillation patterns.

The physical sizes of the acoustic oscillations were directly proportional to their oscillation frequencies. The acoustic peaks in the CMB angular power spectrum correspond to sets of oscillations that just happened to be at extrema in their oscillation cycles at the epoch of last scattering.

Figure 7.4 shows a schematic of how, during the time before the epoch of last scattering, the baryon–photon fluid pressure varied within acoustic oscillations corresponding to the first three acoustic peaks. The first peak corresponds to oscillations that had only just stopped collapsing for the first time and were about to start their expansion phase, while the second peak was produced by smaller oscillations that were about to recollapse after completing their first expansion phase.

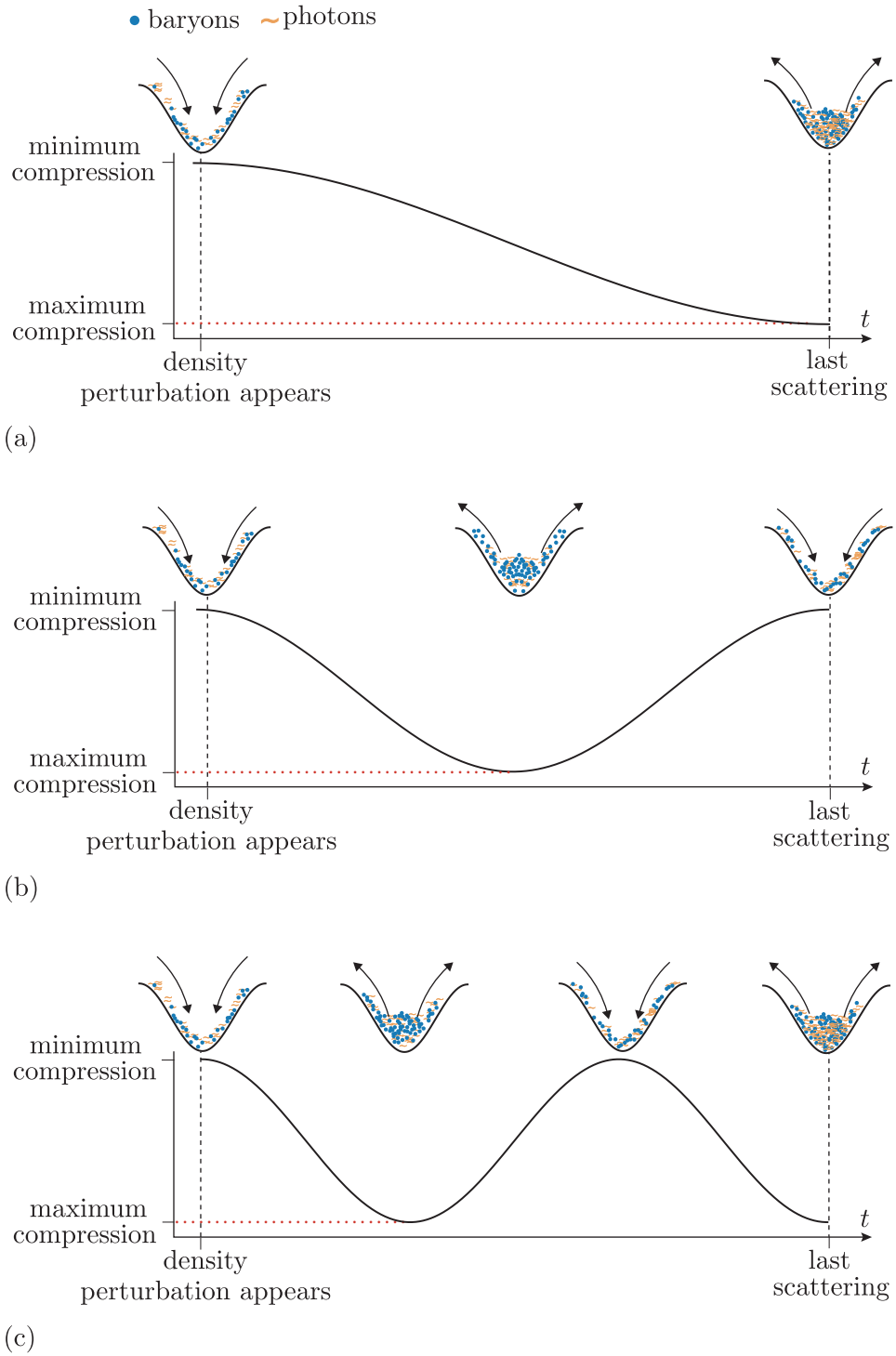

Figure 7.4 Evolution of density over time for three different density perturbations. Panel (a) shows the evolution of density for a perturbation that contributes to the first acoustic peak in the CMB power spectrum; panels (b) and (c) show density perturbations that contribute to the second and third peaks, respectively.

7.1.3 Radiation driving

So far in this section we have focused on the evolution of acoustic oscillations when *dark matter* dominated the energy density of the Universe. Now we briefly discuss the evolution of acoustic oscillations during the short *radiation*-dominated era of the Universe's history and explain how this differs from the dark-matter-dominated case. We will see that radiation dominance can significantly change the way that acoustic oscillations evolve, and we discuss how this impacts the shape of the CMB power spectrum.

For context, bear in mind that the *overall* energy density (sometimes referred to as the background density) decreases as the Universe expands, regardless of whether matter or radiation is dominant. In the matter-dominated case, $\rho \approx \rho_{\rm m} \propto a^{-3}$, whereas if radiation dominates then the density drops even faster, with $\rho \approx \rho_{\rm r} \propto a^{-4}$.

Now, recall that acoustic oscillations evolve within *local* regions that are overdense with respect to the universal average. It turns out that the co-evolution between the gravitational potential of these regions and the densities of the fluids they contain depends strongly on whether the Universe is dominated by matter or radiation. A rigorous mathematical description of the co-evolution between gravitational potential and photon density is quite complicated so we will only provide a qualitative description in this book.

For overdensities and their associated potential wells to persist, they must be able to collapse faster than the expanding Universe can reduce their energy density and wipe them out. During the *matter*-dominated era, the gravitational potential of the overdensities was dominated by the energy density of dark matter. These overdensities could persist and even grow because dark matter has no internal pressure to halt its collapse.

In contrast, during the *radiation*-dominated era, the dark matter, baryons and photons were collapsing due to gravitational potentials that were dominated by the energy density of the photons themselves. The increasing internal pressure of the collapsing photons was able to resist the influence of their self-gravity. This slowed the gravitational collapse and allowed expansion of the Universe to start reducing the *local* energy density of photons such that their associated gravitational potential started to decay.

The important result is that during the radiation-dominated era, the potential wells of the overdensities decayed away completely at almost exactly the same time as the photon pressure completely halted their gravitational collapse. The gravitational potential that had compressed the photons and baryons had vanished, but the fluid was still over-pressured relative to its surroundings and started to expand again. Without a gravitational potential to overcome, the fluid was able to keep expanding until its density was substantially lower than it had been before the collapse began (Figure 7.5). The fluid density then continued to oscillate with an amplitude equivalent to half its rebound level.

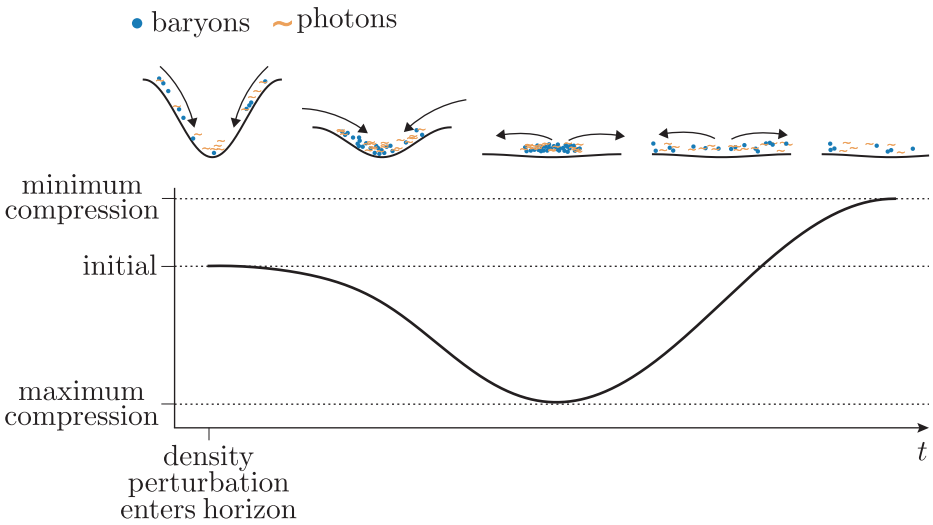

Figure 7.5 Evolution of an acoustic oscillation that becomes encompassed by the particle horizon during the radiation-dominated era of the Universe's history. By the time the photon–baryon fluid reaches maximum compression, the gravitational potential has decayed away and the fluid can rebound to a lower density than it started with.

The overall result is an amplification of acoustic oscillations during the radiation-dominated era, which cosmologists call **radiation driving**. Radiation driving enhances the power spectrum and increases the height of the acoustic peaks for any density perturbations that were smaller than the horizon distance at any point while the Universe's energy density was radiation-dominated.

7.1.4 The origin of the temperature fluctuations

Before we explain how cosmological constraints can be extracted from the CMB power spectrum, we will briefly discuss how the density perturbations that existed at $z_{\rm ls}$ actually produced temperature fluctuations in the CMB.

Consider a population of CMB photons that started their journey to Earth within a dark-matter overdensity at the epoch of last scattering. The gravitational potential of the dark matter redshifts the photons as they propagate out of the overdensity, which makes their spectrum appear cooler. Conversely, CMB photons that were released in underdense regions of the Universe acquired gravitational blueshifts as they fell towards nearby overdensities, making their spectrum appear hotter. This purely gravitational influence on the observed temperatures of CMB photons is called the **Sachs–Wolfe effect** and is the dominant mechanism by which density perturbations that are larger than $d_{\rm hor}(t_{\rm ls})$ can imprint temperature fluctuations on the CMB.

For density perturbations smaller than $d_{\rm hor}(t_{\rm ls})$, the Sachs–Wolfe effect combines with two additional phenomena that also modify the temperature of the CMB photons they produce. The photons and baryons within these *sub-horizon* perturbations were undergoing acoustic oscillations at the epoch of last scattering. Photon fluids that were within the first half of an oscillation cycle had a higher density and were more compressed than the Universal average, while photon fluids in the second half of a cycle had a below-average density.

It is a standard result from thermodynamics that the temperature of a radiation fluid increases as the radiation pressure and energy density increase, such that $T_{\rm r} \propto P_{\rm r}^{1/4} \propto \rho_{\rm r}^{1/4}$. This means that photon fluids that were relatively overdense were hotter than average, while those that were relatively underdense were cooler.

Stefan–Boltzmann law

The energy density ϵ of radiation with temperature T can be calculated using

$$\epsilon = \frac{4\sigma_{\rm SB}T^4}{c} \tag{7.3}$$

where $\sigma_{\rm SB}$ is the Stefan–Boltzmann constant.

The *motion* of the photon–baryon fluid as it oscillates also modifies the apparent temperature of the CMB photons by Doppler-shifting their frequencies. If the fluid was receding from us at the epoch of last scattering, then the photons entrained within it will be redshifted and will therefore appear cooler. Conversely, CMB photons that were released from regions of photon–baryon fluid that were moving towards us will be blueshifted and appear hotter. The combination of these two effects means that for photons within dark-matter density perturbations smaller than $d_{\rm hor}(t_{\rm ls})$, their observed temperature where they appear on the CMB depends on the phase of their acoustic oscillation at the epoch of last scattering.

In practice, the effect of compression heating the photons dominates over the Doppler shift caused by their motion, which is why the acoustic peaks in Figure 7.1 correspond to maxima and minima in the photon-compression cycle and not to the points where the fluid velocities are at their fastest.

Silk damping

For multipole numbers $\ell \gtrsim 2000$, the heights of the peaks in the CMB power spectrum drop away rapidly. This effect is due to a process called **Silk damping**, after astrophysicist Joseph Silk.

In Section 6.1 we mentioned that the Universe did not become transparent instantaneously and so the surface of last scattering is really more like a thin shell. As the opacity of the Universe decreased, the photon–baryon fluid began to decouple and photons were able to travel larger distances before they were scattered by electrons. This allowed them to exchange energy with more distant photons and baryons, which in turn reduced the difference in temperature between nearby density perturbations.

The effect on the CMB is to smear out temperature fluctuations that correspond to physical scales smaller than the thickness of the last-scattering 'shell'. This smearing reduces the variance of the CMB on these scales and suppresses the peaks in the high-ℓ region of the power spectrum.

By measuring the multipole number at which Silk damping manifests, cosmologists can determine how thick the last scattering shell is and, therefore, how long it took for the Universe to become transparent.

7.2 Cosmological parameter measurements

In this section you will finally learn how the observed pattern of CMB temperature fluctuations can provide strong constraints on the cosmological parameters of our Universe.

You already read in Section 6.3.2 that models of the Universe can be used to predict the expected values for different statistical properties of the CMB, including its angular power spectrum C_ℓ. In this section we will spend some time discussing a series of figures that show the effect of varying particular cosmological parameters (Ω_k, $\Omega_{\mathrm{b},0}$, $\Omega_{\mathrm{m},0}$ and $\Omega_{\Lambda,0}$) on the CMB angular power spectrum. By comparing the measured power spectrum with theoretical predictions from models that assume different sets of cosmological parameters, cosmologists can identify the sets of models and model parameters that best fit the observed data.

7.2.1 The acoustic scale

The acoustic oscillations that were described in Section 7.1.2 produce a pattern of fluctuating density and pressure throughout the Universe. Fluctuations in density and pressure are just sound waves, and the pattern of acoustic oscillations can be treated as a superposition of standing sound waves with different wavelengths that correspond roughly to the spacing between neighbouring dark-matter overdensities.

Now, consider a particular acoustic oscillation that contributes to the first acoustic peak in the CMB angular power spectrum. If we could use a

cosmological model to predict the physical size of this oscillation, then we can use Equation 7.1 to compute the expected angular size of the CMB temperature fluctuation it produces. By comparing our predicted angular size with the observed position of the first acoustic peak in the CMB angular power spectrum, we can find a set of parameters for our cosmological model that match those of the real Universe. The calculation required to compute this oscillation's physical size lies outside the scope of this module, but the solution is that it is roughly equal to the **sound horizon** at the epoch of last scattering, which we will denote using the symbol d_s and which can be calculated using:

$$d_\mathrm{s}(z_\mathrm{ls}) = a(z_\mathrm{ls}) \int_0^{t_\mathrm{ls}} \frac{c_\mathrm{s}}{a(t)}\,\mathrm{d}t \tag{7.4}$$

The sound horizon represents the maximum proper distance that a sound wave could have propagated between the big bang and the epoch of last scattering. The speed of sound c_s during this early phase of the Universe's evolution can be calculated using assumed model values for the baryon density parameter Ω_b and the radiation density parameter Ω_r at that time:

$$c_\mathrm{s} = c\left(3 + \frac{9}{4}\frac{\Omega_\mathrm{b}}{\Omega_\mathrm{r}}\right)^{-1/2} \tag{7.5}$$

The second, third and fourth acoustic peaks correspond to oscillations that have physical sizes one-half, one-quarter and one-eighth of $d_\mathrm{s}(z_\mathrm{ls})$, respectively. To get some physical intuition for this result, recall from Section 7.1.2 that oscillations contributing to the first acoustic peak were just about to rebound after their first collapse phase, which began when the primordial density perturbations first appeared in the Universe. Reaching a state of maximum compression implies that a propagating sound wave had time to modify the fluid pressure throughout the whole oscillation, which means that its maximum possible size is roughly equal to the sound horizon.

We can use the angular diameter distance to the surface of last scattering $d_\mathrm{A}(z_\mathrm{ls})$ to calculate a quantity called the **acoustic scale**, which we will denote θ_s and is defined as the observable angular scale of temperature fluctuations contributing to the first acoustic peak in Figure 7.1.

The acoustic scale

$$\theta_\mathrm{s} \approx \frac{d_\mathrm{s}(z_\mathrm{ls})}{d_\mathrm{A}(z_\mathrm{ls})} \tag{7.6}$$

The acoustic scale is one of the most important directly observable properties of the CMB and its value can be used to help constrain several of the cosmological parameters.

Example 7.2

Show that Ω_b remained less than Ω_r until after the epoch of last scattering.

Solution

To solve this problem we first need to compute the redshift z_rb when the energy densities of baryons and radiation were equal. At all higher redshifts, corresponding to smaller scale factors, the radiation energy density would have dominated because $\rho_\mathrm{r} \propto a^{-4}$, whereas the baryon density evolves like matter, that is $\rho_\mathrm{b} \propto a^{-3}$. We want to show that $z_\mathrm{rb} < z_\mathrm{ls}$.

To find z_rb, we start by computing the corresponding scale factor a_rb. Because we know that the densities of baryons and radiation are equal when $a = a_\mathrm{rb}$, we can write:

$$\rho_\mathrm{r}(a_\mathrm{rb}) = \rho_\mathrm{b}(a_\mathrm{rb})$$

Using the density power laws for radiation and matter (baryonic) gives

$$\frac{\rho_{\mathrm{r},0}}{a_\mathrm{rb}^4} = \frac{\rho_{\mathrm{b},0}}{a_\mathrm{rb}^3}$$

and we then divide both sides by the present-day critical density $\rho_{\mathrm{c},0}$ (defined in Equation 4.27):

$$\frac{\rho_{\mathrm{r},0}}{a_\mathrm{rb}^4\,\rho_{\mathrm{c},0}} = \frac{\rho_{\mathrm{b},0}}{a_\mathrm{rb}^3\,\rho_{\mathrm{c},0}}$$

Identifying the ratio of densities on each side as the present-day density parameters and cancelling scale factors gives

$$\frac{\Omega_{\mathrm{r},0}}{a_\mathrm{rb}} = \Omega_{\mathrm{b},0}$$

and so

$$a_\mathrm{rb} = \frac{\Omega_{\mathrm{r},0}}{\Omega_{\mathrm{b},0}}$$

Now we just need to compute z_rb. Using the values listed in the table of constants:

$$\begin{aligned} z_\mathrm{rb} &= \frac{1}{a_\mathrm{rb}} - 1 = \frac{\Omega_{\mathrm{b},0}}{\Omega_{\mathrm{r},0}} - 1 \\ &= \frac{0.0490}{5.4 \times 10^{-5}} - 1 \\ &\approx 910 \end{aligned}$$

As required, this value is less than $z_\mathrm{ls} \approx 1090$ so we have shown that Ω_b remained less than Ω_r until after the epoch of last scattering.

Exercise 7.2

In Example 7.2 you saw that Ω_b remained less than Ω_r until after the epoch of last scattering. This result means that you can assume baryons have a negligible influence on the properties of the photon–baryon fluid, i.e. that $\Omega_\mathrm{r} \gg \Omega_\mathrm{b}$.

(a) Hence, show that the approximation

$$d_\mathrm{s}(z_\mathrm{ls}) \approx \frac{d_\mathrm{hor}(z_\mathrm{ls})}{\sqrt{3}}$$

where $d_\mathrm{hor}(z_\mathrm{ls})$ is the horizon distance at t_ls (when photons with observed redshift z_ls were emitted), is a good one.

(b) Now use this approximation and the fact that $d_\mathrm{A}(z_\mathrm{ls}) = 12.73\,\mathrm{Mpc}$ to estimate the multipole ℓ_s that corresponds to the acoustic scale in the CMB power spectrum; you may assume the result from Example 7.1 that $d_\mathrm{hor}(z_\mathrm{ls}) = 0.29\,\mathrm{Mpc}$.

Your answer should be very close to the *observed* location of the first peak in Figure 7.1.

7.2.2 Measuring Ω_k

We end this chapter with some examples of cosmological parameters that can be constrained using the properties of the CMB angular power spectrum.

Let's consider the measured location of the first acoustic peak, which corresponds to the acoustic scale and can be used to constrain the *curvature* of the Universe. As discussed in Chapter 5, curvature affects the measured angular sizes for objects of a fixed physical size. This includes the CMB acoustic peaks, whose physical scale is fixed by the physics discussed in the previous section. The predicted effect of spatial curvature on the CMB power spectrum is shown in Figure 7.6. Increasing the value of the density parameter for curvature, Ω_k, makes temperature fluctuations seem smaller and moves all of the acoustic peaks to higher values of ℓ.

- Bearing in mind the curves shown in Figure 7.6, is the CMB power spectrum measured by *Planck* compatible with $\Omega_k < -0.2$?
- No. Notwithstanding the fact that the predicted peak positions do not match their observed counterparts, values of $\Omega_k < -0.2$ predict a very large rise at low values of ℓ that is strongly disfavoured by the observed data, which are plotted in Figure 7.1.

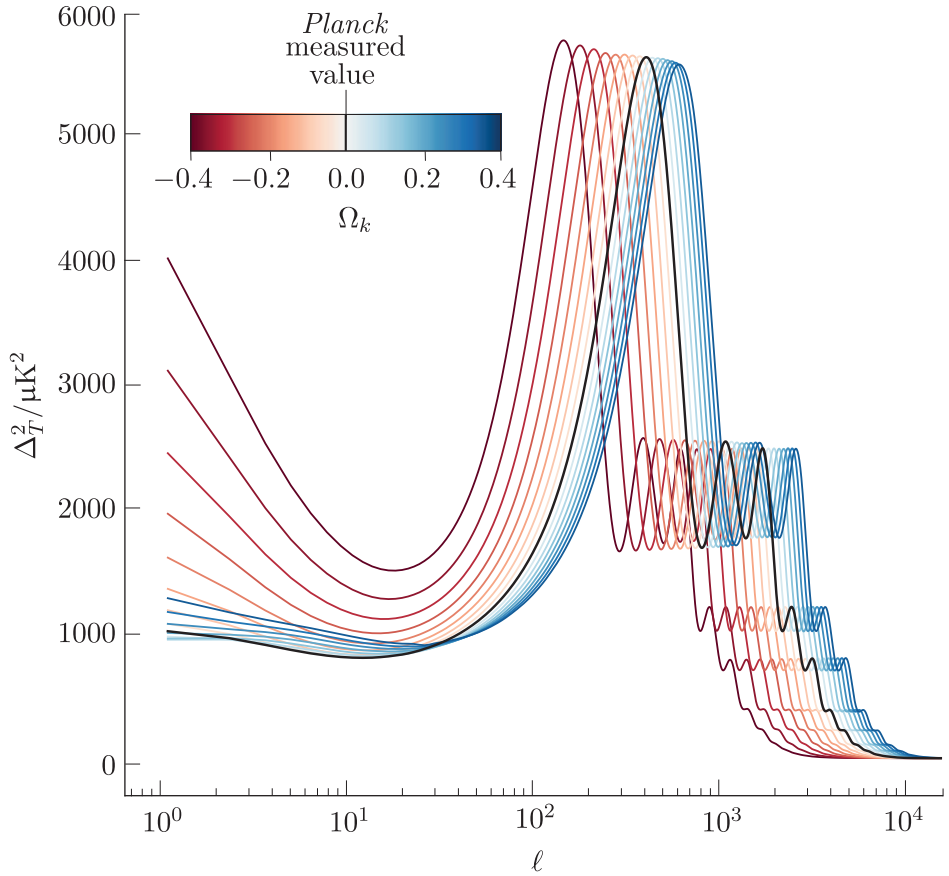

Figure 7.6 Effect of varying Ω_k on the CMB power spectrum. The value of Ω_k derived from *Planck*'s measurements is shown as a solid black line; all other cosmological parameters are fixed to the values listed in the table of constants.

The value for $d_\mathrm{A}(z_\mathrm{ls}) = 12.73\,\mathrm{Mpc}$ that you assumed in Exercise 7.2 assumes a flat universe with $\Omega_k = 0$. The fact that the position you estimated for the first acoustic peak agrees so well with observation is compelling evidence that the real Universe is indeed spatially flat.

The precise positions of the acoustic peaks in Figure 7.1 also depend somewhat on the relative densities of photons and baryons in the Universe at and before the epoch of last scattering. This is because both Ω_b and Ω_r appear in the definition of the speed of sound in Equation 7.5. Unless we can find a way to independently constrain $\Omega_\mathrm{b}/\Omega_\mathrm{r}$, this additional dependency will limit how tightly we can constrain Ω_k. There might be several different sets of values for Ω_b, Ω_r and Ω_k that predict very similar locations for the acoustic peaks and we would have no way of knowing which set was true! Fortunately, the CMB power spectrum *itself* provides another, largely independent way to determine Ω_b, by comparing the *amplitudes* of the different acoustic peaks. We discuss this further in the next section.

7.2.3 Measuring $\Omega_{\mathrm{b},0}$

In this section we will discuss how observations of the CMB power spectrum can also be used to constrain the *baryonic* matter density parameter $\Omega_{\mathrm{b},0}$.

Figure 7.7 shows how changing the value of $\Omega_{\mathrm{b},0}$, while keeping the values of $\Omega_{\mathrm{m},0}$, $\Omega_{\Lambda,0}$ and H_0 fixed to the values in the table of constants, affects the *relative* heights of the acoustic peaks. A higher baryon fraction enhances the first and third acoustic peaks, but reduces the height of the second.

Constraints on the density parameters that are derived from CMB data alone are often presented as multiples of h^2 where h represents the Hubble constant, H_0, in units of $100\,\mathrm{km\,s^{-1}\,Mpc^{-1}}$.

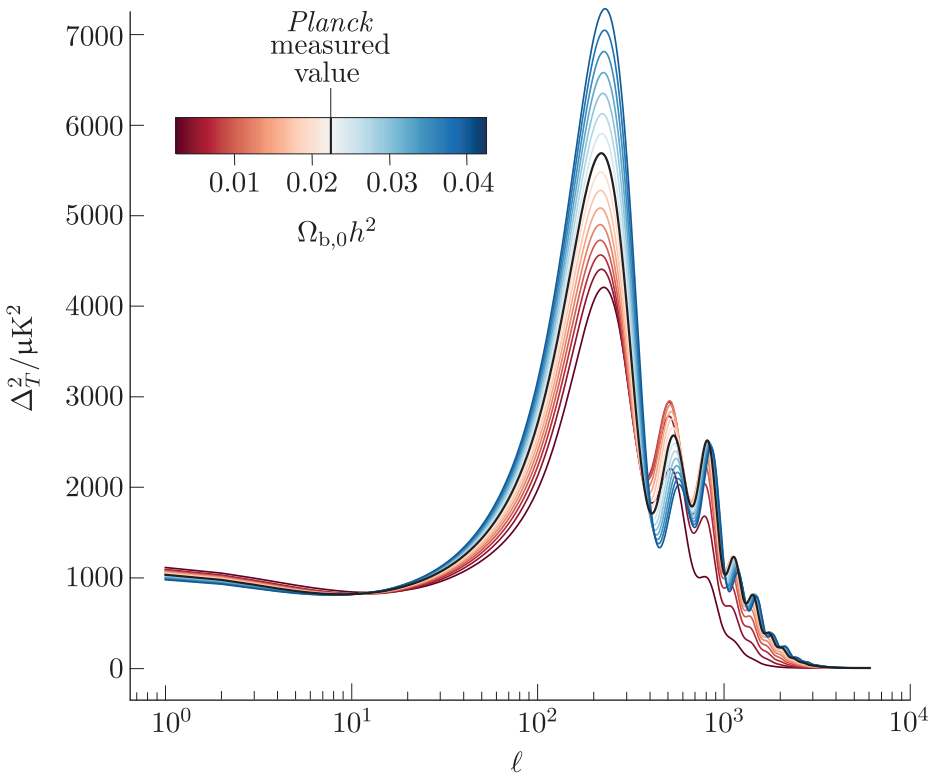

Figure 7.7 The effect of varying $\Omega_{\mathrm{b},0}$ on the CMB power spectrum. The value of $\Omega_{\mathrm{b},0}$ derived from *Planck*'s measurements is shown as a solid black line; all other cosmological parameters are fixed to the values listed in the table of constants.

To understand these effects we need to recognise that adding baryons to the photon–baryon fluid increases its mass but does not change its pressure. This is because baryons are matter and have sufficiently low density that their equation of state parameter $w_{\mathrm{b}} = 0$ (see Chapter 4). A useful analogy for the effect of increasing Ω_{b} is illustrated in Figure 7.8. The oscillating photon–baryon fluid behaves in a similar way to a mass attached to a spring, oscillating in the vertical direction under gravity. The spring represents the radiation pressure counteracting the gravitational influence of the dark-matter overdensity.

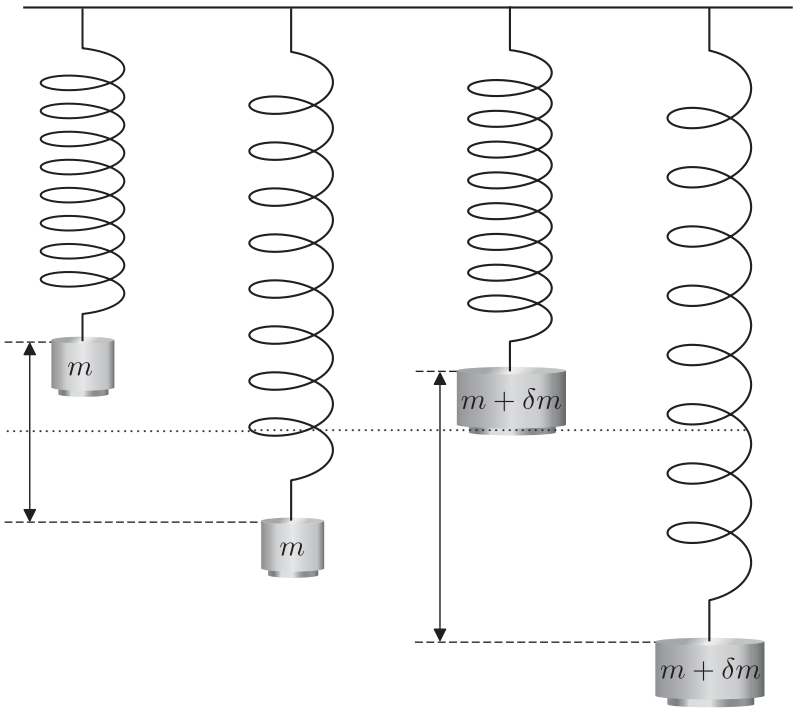

Figure 7.8 Masses oscillating on a spring. Increasing the mass while leaving the spring unchanged is analogous to increasing the density of baryons in an acoustic oscillation. The effect is to increase the amplitude of the oscillations (shown by the vertical arrows) and also to lower their midpoint. The dotted line represents the oscillation midpoint of the smaller mass and is analogous to the mean density of the Universe.

Increasing the size of the mass while leaving the spring unchanged has two effects on the oscillations it undergoes. First, the mass falls further before the spring can arrest its motion, so the amplitude of the oscillations increases. In a similar way, a more massive photon–baryon fluid will sink deeper into the gravitational potential of a dark-matter overdensity before its internal pressure can halt its collapse. This means that when the fluid reaches its maximum compression, it will be denser and the photons within it will have a higher temperature.

- Does this mean that we should expect to see more CMB hot spots than cold spots in a Universe that contains more baryons?
- No. Remember that for every potential well that fills up with photons and baryons there is a corresponding potential hill that drains away. If the fluid in the wells becomes more compressed, then the fluid on the hills must become even more rarefied.

Most importantly, the *difference* between the temperature of the oscillations that are at maximum compression and the average temperature of the Universe is larger if the Universe contains more baryons. This increases the contribution to the variance of the CMB of oscillations that had reached maximum compression at the epoch of last scattering, which enhances the angular power spectrum on angular scales that correspond to the odd-numbered acoustic peaks.

The second impact of increasing the mass attached to the spring is that the midpoint of the oscillation, where the speed of the mass is greatest, moves lower. A similar effect modifies the acoustic oscillations. During the expansion phase of the acoustic oscillations the pressure from photons in the fluid must now overcome the added inertia from the extra baryons. This means that the fluid will not rebound as far, and oscillations that had reached their maximum rarefaction at the epoch of last scattering will have photon temperatures that are closer to the Universal average. The result of adding more baryons to the Universe is that the even-numbered peaks in the CMB angular power spectrum are suppressed.

Figure 7.9 shows a comparison of how the density of an acoustic oscillation within a potential well evolves for fluids that contain baryons and for those that do not.

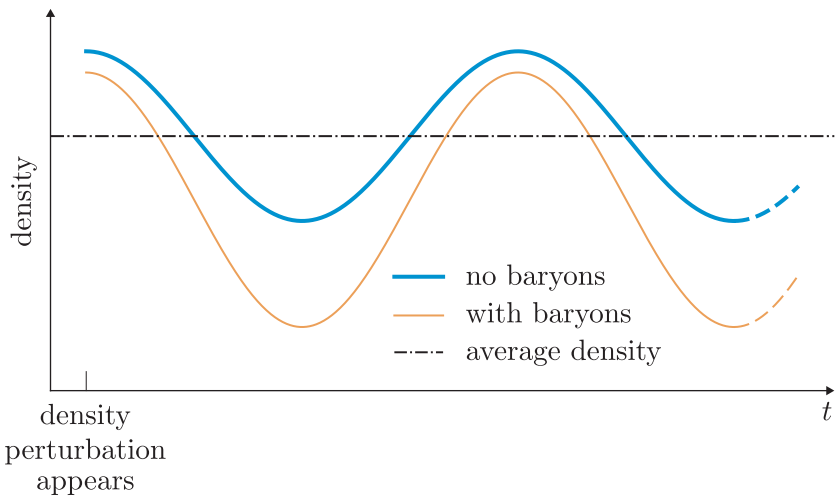

Figure 7.9 The evolution of density in a potential *well* before t_{ls} for fluids that contain baryons (orange) and those that do not (blue). Adding baryons increases the amplitude of the oscillations and lowers the oscillation midpoint with respect to the average density of the Universe (dot-dashed line).

- If adding baryons increases the maximum pressure and temperature of the photon–baryon fluid in the potential wells, why don't the average temperature and density of the Universe also go up?
- Again, we need to remember that every potential well has a corresponding potential hill. If baryons and photons sink deeper into a potential well, they fall further from the potential hill, leaving it more rarefied and therefore cooler. The temperature and density changes in the wells and on the hills balance each other out, so the *average* temperature and density stay the same.

By measuring the heights *and* positions of the acoustic peaks observed by the *Planck* satellite, cosmologists are able to very precisely constrain the product $\Omega_{b,0}h^2 = 0.022\,42 \pm 0.000\,14$, where h represents the Hubble constant, H_0, in units of $100\,\mathrm{km\,s^{-1}\,Mpc^{-1}}$.

7.2.4 Measuring $\Omega_{\mathrm{m},0}$

In this section we will discuss how observations of the CMB power spectrum can also be used to constrain the *overall* matter density parameter $\Omega_{\mathrm{m},0}$.

Figure 7.10 shows the effect that changing $\Omega_{\mathrm{m},0}$ has on the CMB power spectrum. Increasing $\Omega_{\mathrm{m},0}$ decreases the amplitude of the acoustic peaks, while decreasing $\Omega_{\mathrm{m},0}$ has the opposite effect. This variation is caused by the radiation-driving phenomenon that you read about in Section 7.1.3.

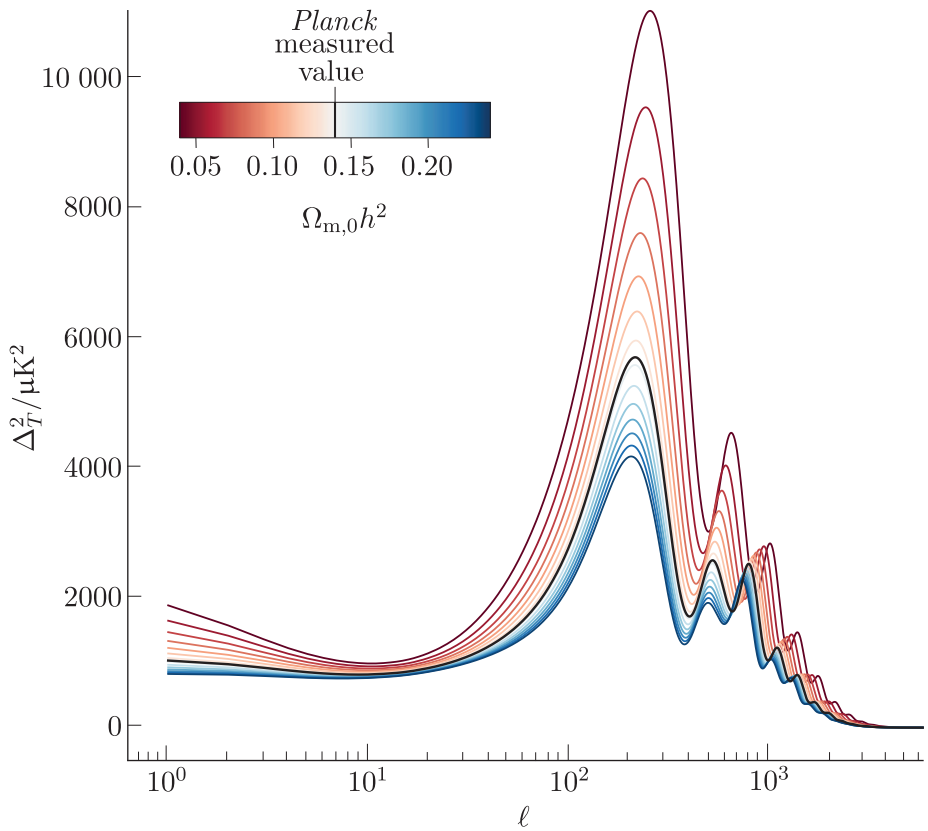

Figure 7.10 Effect of varying $\Omega_{\mathrm{m},0}$ on the CMB power spectrum. The value of $\Omega_{\mathrm{m},0}$ derived from *Planck*'s measurements is shown as a solid black line; all other cosmological parameters are fixed to the values listed in the table of constants.

- What percentage of *matter* in the Universe is baryonic? What other type of matter constitutes the remainder?
- You may recall from Chapter 1 that about 17% of matter in the Universe is baryonic. The rest is non-baryonic dark matter.

The primary effect of increasing $\Omega_{\mathrm{m},0}$ is to increase the amount of dark matter within overdensities. During the radiation-dominated era of the Universe's history, this helped to stabilise them and prevent potential wells from decaying away completely. The residual gravitational potentials reduce the rebound amplitude of the acoustic oscillations, thereby reducing

the heights of the acoustic peaks. Decreasing $\Omega_{\mathrm{m},0}$ has the opposite effect: potential wells decay away more quickly, leaving them shallower and allowing acoustic oscillations to expand further and reach lower densities when they rebound.

- Would you expect radiation driving to amplify the CMB power spectrum on all angular scales?
- No. Only oscillations that were smaller than the horizon distance during the radiation-dominated era of the Universe's history would be amplified. This means that oscillations larger than the angular scale corresponding to the horizon distance at the epoch of matter–radiation equality would not be amplified.

Varying the overall matter density also shifts the *positions* of the acoustic peaks by changing the size of the sound horizon at the epoch of last scattering. By accounting for the observed positions and amplitudes of the acoustic peaks, the CMB power spectrum can be used to constrain $\Omega_{\mathrm{m},0}h^2$ to within 2%.

7.2.5 Measuring $\Omega_{\Lambda,0}$

Finally in this section we consider the energy density of the cosmological constant. We will find that CMB data *on their own* can only provide very weak constraints on $\Omega_{\Lambda,0}$ and we will discuss why this is the case.

Figure 7.11 shows that large changes in $\Omega_{\Lambda,0}$ produce minimal variations in either the positions *or* the amplitudes of the acoustic peaks in the CMB power spectrum.

The main reason that the value of $\Omega_{\Lambda,0}$ has so little influence on the CMB power spectrum is that the energy density of the cosmological constant was completely negligible compared to those of matter and radiation during the time before t_{ls}, when the acoustic oscillations were evolving. The following example demonstrates the huge dominance of matter and radiation over Λ prior to the epoch of last scattering.

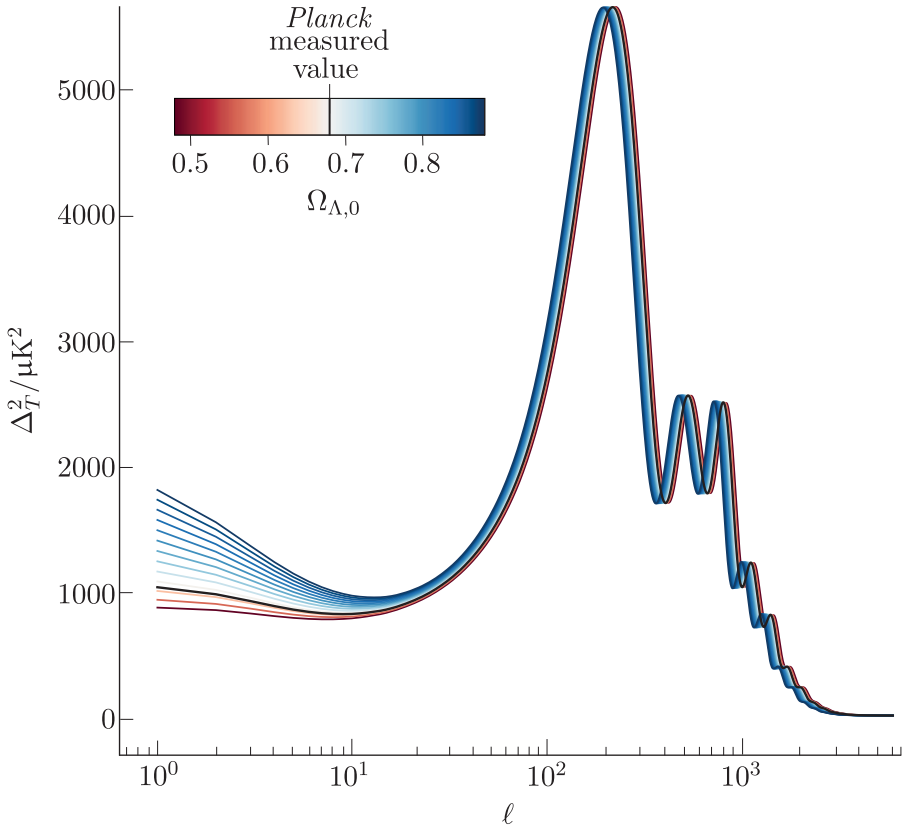

Figure 7.11 Effect of varying $\Omega_{\Lambda,0}$ on the CMB power spectrum. The value of $\Omega_{\Lambda,0}$ derived from *Planck*'s measurements is shown as a solid black line; all other cosmological parameters are fixed to the values listed in the table of constants.

Example 7.3

(a) Using the values listed in the table of constants, compute the values of $\Omega_\mathrm{m}/\Omega_\mathrm{r}$ and $\Omega_\mathrm{m}/\Omega_\Lambda$ at the epoch of last scattering, assuming $z_\mathrm{ls} = 1090$.

(b) How would these ratios evolve for even higher redshifts?

Solution

(a) To solve this problem we can relate the ratios of the present-day density parameters to their values at z_ls. We first need to recall from Chapter 4 how the density of each component evolves as the Universe expands:

$$\rho_\mathrm{m} = \rho_{\mathrm{m},0}a^{-3} = \rho_{\mathrm{m},0}(1+z)^3$$
$$\rho_\mathrm{r} = \rho_{\mathrm{r},0}a^{-4} = \rho_{\mathrm{r},0}(1+z)^4$$
$$\rho_\Lambda = \rho_{\Lambda,0}$$

Now we can compute the required ratios:

$$\frac{\Omega_{\rm m}(z_{\rm ls})}{\Omega_{\rm r}(z_{\rm ls})} = \frac{\rho_{\rm m}(z_{\rm ls})/\rho_{\rm c}(z_{\rm ls})}{\rho_{\rm r}(z_{\rm ls})/\rho_{\rm c}(z_{\rm ls})} = \frac{1}{1+z_{\rm ls}}\frac{\rho_{\rm m,0}}{\rho_{\rm r,0}} = \frac{1}{1+z_{\rm ls}}\frac{\Omega_{\rm m,0}}{\Omega_{\rm r,0}}$$

and

$$\frac{\Omega_{\rm m}(z_{\rm ls})}{\Omega_{\Lambda}(z_{\rm ls})} = \frac{\rho_{\rm m}(z_{\rm ls})/\rho_{\rm c}(z_{\rm ls})}{\rho_{\Lambda}(z_{\rm ls})/\rho_{\rm c}(z_{\rm ls})} = (1+z_{\rm ls})^3\frac{\rho_{\rm m,0}}{\rho_{\Lambda,0}} = (1+z_{\rm ls})^3\frac{\Omega_{\rm m,0}}{\Omega_{\Lambda,0}}$$

The final steps in each of the previous two expressions replace the ratio of present-day densities with the (equivalent) ratio of present-day density parameters. Using the values from the table of constants, we find

$$\frac{\Omega_{\rm m}(z_{\rm ls})}{\Omega_{\rm r}(z_{\rm ls})} = \frac{1}{1+z_{\rm ls}}\frac{\Omega_{\rm m,0}}{\Omega_{\rm r,0}} = \frac{1}{1091}\frac{0.3097}{5.4\times10^{-5}} = 5.3$$

and

$$\frac{\Omega_{\rm m}(z_{\rm ls})}{\Omega_{\Lambda}(z_{\rm ls})} = (1+z_{\rm ls})^3\frac{\Omega_{\rm m,0}}{\Omega_{\Lambda,0}} = (1091)^3\frac{0.3097}{0.6888} = 5.84\times10^8$$

(b) The density of matter grows more slowly with redshift than the density of radiation does. Therefore at higher redshifts the value of $\Omega_{\rm m}/\Omega_{\rm r}$ would decrease and fall below 1 at $z_{\rm mr}$, when the energy densities of matter and radiation become equal. Conversely, $\Omega_{\rm m}/\Omega_{\Lambda}$ would continue to increase all the way back to the big bang.

Bearing in mind the results that are derived in Example 7.3, the Friedmann equation tells us that the value of $\Omega_{\Lambda,0}$ has almost no influence on the expansion of the Universe during the time before the epoch of last scattering. As a consequence, the cosmological constant barely affects physical scales that impact the CMB power spectrum (e.g. the sizes of the sound horizon and the particle horizon) and it does not enhance or diminish the radiation-driving effect.

In addition to being very small, the effect of varying $\Omega_{\Lambda,0}$ on the CMB power spectrum is almost identical to the effect of varying Ω_k. Both parameters shift the locations of the peaks without changing their relative spacing or substantially changing their amplitudes. A very small amount of curvature can replicate large changes in the energy density of Λ, which means that it is impossible to *simultaneously* derive precise constraints on $\Omega_{\Lambda,0}$ and Ω_k using CMB data *alone*.

7.2.6 Cosmological parameter degeneracies and combined constraints

In the previous section you saw how observations of the CMB can be used to provide strong constraints on many of the cosmological parameters. However, you also saw that models with different sets of input parameters can predict CMB power spectra with very similar observable characteristics, and that varying different parameters can sometimes

modify those predictions in very similar ways. Such correlations between the effects of different parameters on the output of a model are called **parameter degeneracies**, and the parameters that produce the correlation are said to be **degenerate**.

Degeneracies between the cosmological parameters limit our ability to precisely constrain their values using observational data, no matter how exquisite those data are. For example, consider the orange region in Figure 7.12a, which highlights the ranges of $\Omega_{\mathrm{m},0}$ and $\Omega_{\Lambda,0}$ that are consistent with CMB observations made using the *WMAP* telescope. The overall extent of this region in the horizontal and vertical directions indicates the precision of the parameter constraints that the *WMAP* data provide; a smaller extent in either direction implies a more precise constraint on the corresponding cosmological parameter.

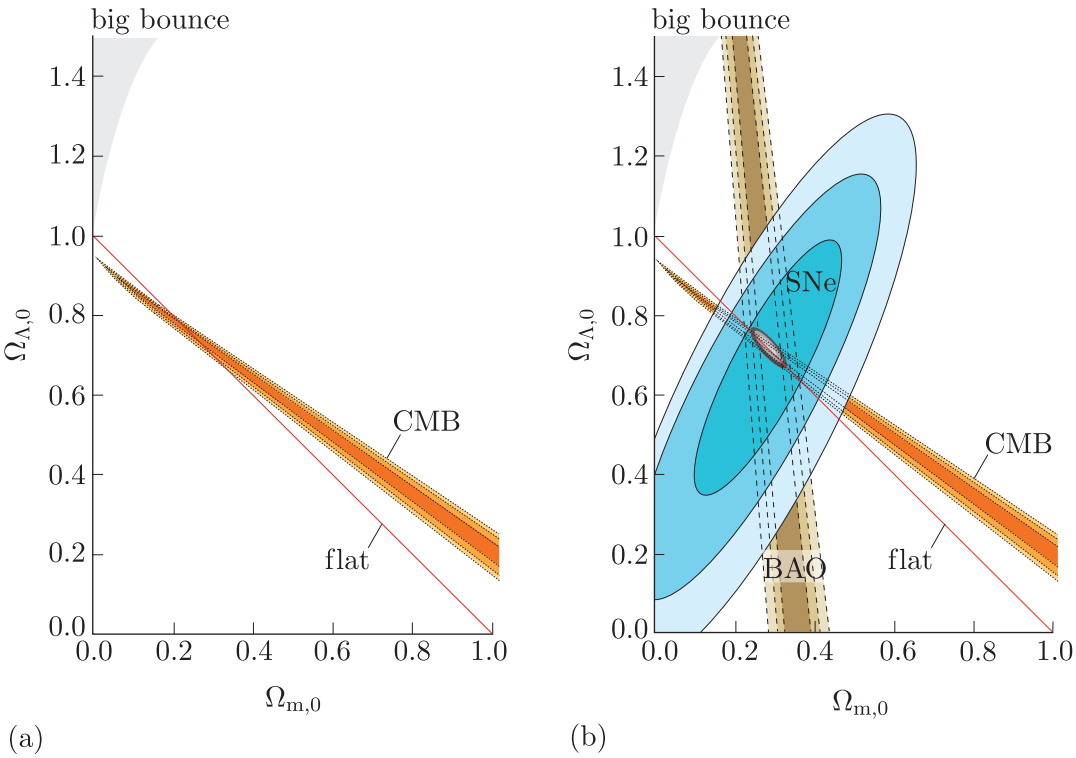

Figure 7.12 (a) Constraints on $\Omega_{\mathrm{m},0}$ and $\Omega_{\Lambda,0}$ derived using observations of the CMB power spectrum on its own (orange contours). (b) Constraints on $\Omega_{\mathrm{m},0}$ and $\Omega_{\Lambda,0}$ derived using observations of Type Ia supernovae (SNe; blue contours), baryon acoustic oscillations (BAO; brown contours) *and* the CMB (orange contours). The small grey oval in (b) shows the region of joint agreement between all three observational measurements. In both panels, the different contour levels indicate regions of decreasing uncertainty, from 3σ (lightest tone) to 2σ and 1σ (darkest).

The orange region is very narrow because for any *specific* value of $\Omega_{\mathrm{m},0}$ (or $\Omega_{\Lambda,0}$), there is a very small range of $\Omega_{\Lambda,0}$ (or $\Omega_{\mathrm{m},0}$) values that are permitted by the *WMAP* data. However, the region is also very extended and spans a large range of parameter values because the values of $\Omega_{\mathrm{m},0}$ and

$\Omega_{\Lambda,0}$ are both *degenerate* with several other cosmological parameters in terms of their effect on the predicted CMB power spectra, primarily Ω_k, $\Omega_{\mathrm{b},0}$ and H_0. Varying the value of $\Omega_{\mathrm{m},0}$ does change the predicted shape of the power spectrum, but this change can be almost completely undone by choosing appropriate values of $\Omega_{\Lambda,0}$, Ω_k, $\Omega_{\mathrm{b},0}$ and H_0.

- Look again at Figures 7.6, 7.10 and 7.11. What property of the CMB power spectrum is similarly affected by variations in Ω_k, $\Omega_{\mathrm{m},0}$ and $\Omega_{\Lambda,0}$ that might therefore be contributing to the degeneracy among these parameters?
- The *positions* of the acoustic peaks are similarly affected; increasing either $\Omega_{\mathrm{m},0}$ *or* $\Omega_{\Lambda,0}$ shifts the peaks to lower multipoles, but this shift can be undone by increasing Ω_k.

There are several techniques that can be used to reduce or circumvent the degeneracies between different cosmological parameters. Such techniques are said to *break* the degeneracies and they allow cosmologists to constrain the cosmological parameters much more precisely.

One commonly used way to break degeneracies in a model with a large number of parameters is to fix one or more of those parameters to particular values. For example, we have already seen in Section 7.2.5 that Ω_k and $\Omega_{\Lambda,0}$ are degenerate parameters that shift the acoustic peaks in a similar way. However, if we *assume* a flat Universe with $\Omega_k = 0$, then we can break this degeneracy and derive a good constraint on $\Omega_{\Lambda,0}$. The solid red diagonal line (labelled 'flat') in the panels of Figure 7.12 identifies the values of $\Omega_{\mathrm{m},0}$ and $\Omega_{\Lambda,0}$ that are consistent with a spatially flat Universe. It represents the Friedmann equation (Equation 4.40) for a Universe with zero curvature and negligible $\Omega_{\mathrm{r},0}$:*

$$1 = \Omega_{\mathrm{m},0} + \Omega_{\Lambda,0} + \Omega_{\mathrm{r},0} \approx \Omega_{\mathrm{m},0} + \Omega_{\Lambda,0} \tag{7.7}$$

The assumption of a flat Universe reduces the set of permissible parameter values to the small range in which the red line intersects the orange contours. If Ω_k is assumed to be zero, then the *WMAP* satellite data constrain $\Omega_{\Lambda,0}$ to be 0.679 ± 0.013.

Even if cosmological parameters are degenerate with respect to their effect on the CMB, it is often possible to break those degeneracies using auxiliary constraints that are derived from observations of phenomena other than the CMB. For example, in Chapter 5 you learned that observations of Type Ia supernovae and measurements of baryon acoustic oscillations (BAOs) can also be used to place constraints on the values of $\Omega_{\mathrm{m},0}$ and $\Omega_{\Lambda,0}$. Figure 7.12b shows these constraints, together with those that can be derived using CMB observations.

The different observational constraints exclude different possible values of $\Omega_{\mathrm{m},0}$ and $\Omega_{\Lambda,0}$. The resultant combined constraints are indicated by the small grey area in Figure 7.12b, which lies at the centre of the region

*$\Omega_{\mathrm{r},0}$ is much smaller than either $\Omega_{\mathrm{m},0}$ or $\Omega_{\Lambda,0}$ so it can usually be neglected in practice. Otherwise, its value is strongly constrained by the observed average CMB temperature.

where the three independent observational constraints overlap. Notice that this grey area coincides closely with the solid red line even though no prior assumptions have been made about the value of Ω_k. The combined data from the CMB, supernovae and BAOs provide strong *observational* evidence that the Universe is indeed flat, and they constrain Ω_k extremely precisely, to a value of 0.0007 ± 0.0019.

In this chapter you have seen that the CMB encodes a wealth of information about the cosmological parameters and the physics of the early Universe. However, it is only by *combining* the CMB observations with complementary observational datasets that the exquisitely precise constraints listed in the table of constants can be obtained. It is often said that we are now living in an age of 'precision cosmology'. Access to such precise measurements allows us to thoroughly test our theoretical models of the Universe and search for evidence of new, unexpected physical processes and phenomena.

7.3 Summary of Chapter 7

- The positions and amplitudes of the **acoustic peaks** in the CMB angular power spectrum reflect the physical sizes and amplitudes of acoustic oscillations at the epoch of last scattering.
- The physical sizes and amplitudes of the acoustic oscillations depend on the speed of sound and physical conditions in the early Universe, which in turn depend on the values of the cosmological parameters. This means that the observed positions and amplitudes of the acoustic peaks in the CMB angular power spectrum depend indirectly, but predictably, on the values of the cosmological parameters.
- Precise measurement and careful analysis of the CMB angular power spectrum can be used to constrain the values of several cosmological parameters, including $\Omega_{\mathrm{b},0}$, $\Omega_{\mathrm{m},0}$ and $\Omega_{\Lambda,0}$.
- Some cosmological parameters affect the predicted CMB angular power spectrum in very similar ways. These groups of parameters are said to be **degenerate**. In particular, $\Omega_{\Lambda,0}$, $\Omega_{\mathrm{m},0}$ and Ω_k are degenerate with respect to their effect on the predicted CMB power spectrum. This degeneracy weakens the constraints on these parameters that can be *simultaneously* derived from CMB observations *alone*.
- **Parameter degeneracies** can be broken by assuming specific values for certain cosmological parameters. For example, assuming that $\Omega_k = 0$ breaks the degeneracy between $\Omega_{\Lambda,0}$ and $\Omega_{\mathrm{m},0}$.
- The degeneracy between $\Omega_{\Lambda,0}$, $\Omega_{\mathrm{m},0}$ and Ω_k can also be broken via complementary constraints derived from observations of Type Ia supernovae and/or baryon acoustic oscillations.